Asymmetric quantum hypothesis testing with Gaussian states

Gaetana Spedalieri and Samuel L. Braunstein
Department of Computer Science, University of York, York YO10 5GH, United Kingdom

We consider the asymmetric formulation of quantum hypothesis testing, where two quantum hypotheses have different associated costs. In this problem, the aim is to minimize the probability of false negatives and the optimal performance is provided by the quantum Hoeffding bound. After a brief review of these notions, we show how this bound can be simplified for pure states. We then provide a general recipe for its computation in the case of multimode Gaussian states, also showing its connection with other easier-to-compute lower bounds. In particular, we provide analytical formulae and numerical results for important classes of one- and two-mode Gaussian states.

PACS numbers: 03.67.-a, 89.70.Cf, 03.67.Hk, 03.65.Ta, 02.10.Ud

arXiv:1407.0884v3 [quant-ph] 3 Sep 2015

I. INTRODUCTION

Quantum hypothesis testing (QHT) is a fundamental topic in quantum information theory [1, 2], playing a non-trivial role in protocols of quantum communication and quantum cryptography [3, 4]. The typical formulation of QHT is given in terms of quantum state discrimination [5–8], where a certain number of generally non-orthogonal quantum states (the quantum hypotheses) have to be discriminated by means of a quantum measurement. In particular, the simplest scenario regards the statistical discrimination between two non-orthogonal quantum states, corresponding to the 'null' and the 'alternative' quantum hypotheses, occurring with some a priori probabilities. In *symmetric testing*, these hypotheses have the same cost [6–8] and the goal is to minimize the mean error probability of confusing them by suitably optimizing the quantum measurement.

For such a basic problem, we know closed analytical formulae identifying both the minimum error probability, given by the Helstrom bound [6], and the optimal quantum detection, expressed in terms of the Helstrom matrix [6]. Furthermore, we can also use an easier-to-compute bound which becomes tight in asymptotic conditions. This is the recently-introduced quantum Chernoff bound [9], for which we know simple formulae in the case of multi-mode Gaussian states [10], (i.e., those states with Gaussian Wigner function [5]).

In this paper, we consider *asymmetric* QHT, where two quantum hypotheses have different associated costs [6–8]. In this approach, we aim to minimize the probability that the alternative hypothesis is confused for the null hypothesis, an error which is known as 'false negative'. This minimization has to be done by suitably constraining the probability of another possible error, known as a 'false positive', where the null hypothesis is confused for the alternative hypothesis. This is clearly the best approach for instance in medical-type testing, where the null hypothesis typically represents absence of a disease, while the alternative corresponds to the presence of a disease.

Asymmetric QHT is typically formulated as a multi-copy discrimination problem, where a large number of copies of the two possible states are prepared and subjected to a collective quantum measurement. From this point of view, the aim is to maximize the error-exponent describing the exponential decay of the false negatives, while placing a reasonable constraint on the false positives. For this calculation, we can rely on two mathematical tools. The first is the quantum relative entropy [5] between the two states, while the other is the recently-introduced quantum Hoeffding bound (QHB) [11], which performs the optimization of the error-exponent while providing a better control on the false positives.

In this work, we start by giving some basic notions on asymmetric QHT and briefly reviewing the QHB, also showing how its computation simply reduces to the quantum fidelity [12] in the presence of pure states. Then, we provide a general recipe for computing this bound in the case of multimode Gaussian states, for which it can be expressed in terms of their first- and second-order statistical moments. In the general multimode case, we derive a relation between the QHB and other easier-to-compute bounds, which are based on well-known mathematical inequalities. Finally, we derive analytical formulas and numerical results for the most important classes of one-mode and two-mode Gaussian states.

By developing the theory of asymmetric QHT for Gaussian states, our work could be useful in tasks and protocols involving Gaussian quantum information [5], including technological applications of quantum channel discrimination (e.g., quantum illumination [13, 14] or quantum reading [15–18]) where we are interested in increasing our ability to accept one specific quantum hypothesis.

II. BRIEF REVIEW OF ASYMMETRIC TESTING

A. Basic formulation

In binary QHT we consider a quantum system which is prepared in some unknown quantum state ρ, which can be ρ_0 or ρ_1. For instance we can imagine one party, say Alice, who prepares such a system. This system is then

passed to Bob, who does not know which choice Alice has made. Thus, Bob must decide between the following two hypotheses

$$\text{Null hypothesis } H_0 : \rho = \rho_0 \ , \tag{1}$$
$$\text{Alternative hypothesis } H_1 : \rho = \rho_1 \ . \tag{2}$$

In order to discriminate between these two hypotheses, i.e., distinguish between the two states, Bob applies a quantum measurement, generally described by a positive operator valued measure (POVM). Without loss of generality, Bob can always reduce his measurement to be a dichotomic POVM $\{\Pi_k\}$ with $k = 0, 1$ [6]. The outcome $k = 0$, with POVM operator Π_0, is associated to the null hypotheses H_0, while the other outcome $k = 1$, with POVM operator $\Pi_1 = I - \Pi_0$, is associated with the alternative hypothesis H_1.

Since the two quantum states ρ_0 and ρ_1 are generally non-orthogonal, there is a non-zero error probability to confuse the two hypotheses. We can identify two different types of error: Type-I and type-II errors, with associated conditional error probabilities. By definition, the type-I error, also known as a 'false-positive', is where Bob accepts the alternative hypothesis H_1 when the null hypothesis H_0 holds. We have a corresponding error probability expressed by

$$\alpha := p(H_1|H_0) = \text{Tr}(\Pi_1 \rho_0). \tag{3}$$

Then, the type-II error or 'false-negative' is where Bob accepts the null hypothesis H_0 when the true hypothesis is the alternative H_1. This error occurs with conditional probability

$$\beta := p(H_0|H_1) = \text{Tr}(\Pi_0 \rho_1). \tag{4}$$

Note that we can introduce other probabilities, but they are fully determined by α and β. For instance, we may also consider the 'specificity' or 'true-negativity' of the test which is the success probability of identifying the null hypothesis, i.e., $p(H_0|H_0)$ which is simply given by $1 - \alpha$. Similarly, we may also consider the 'sensitivity' or 'true-positivity' of the test which is the success probability of identifying the alternative hypothesis, i.e., $p(H_1|H_1) = 1 - \beta$.

The costs associated with the two types of error can be very different especially in the medical and histological settings. For instance, in a medical test, H_0 is typically associated with no illness, while H_1 with the presence of the disease. It is therefore clear that we would like to have tests where the false-negative probability (or rate) β is the lowest possible, so that ill patients are not diagnosed as healthy. For this reason, in a medical setting, hypothesis testing is almost always asymmetric, meaning that we aim to minimize one of the two conditional error probabilities.

B. Multi-copy formulation

In general we can formulate the problem of QHT as an M-copy discrimination problem [7, 8]. This means that Alice has M quantum systems which are prepared in two possible multi-copy states

$$H_0 : \rho = \rho_0^{\otimes M} = \rho_0 \otimes ... \otimes \rho_0 \ , \tag{5}$$
$$H_1 : \rho = \rho_1^{\otimes M} = \rho_1 \otimes ... \otimes \rho_1 \ .$$

These systems are passed to Bob who performs a collective measurement on them. As before, this general POVM can be chosen to be dichotomic $\{\Pi_0, \Pi_1\}$ with $\Pi_1 = I - \Pi_0$.

The error probabilities now depend on the number of copies M. In particular, the probability of false positives is given by

$$\alpha_M := p(H_1|H_0) = \text{Tr}(\Pi_1 \rho_0^{\otimes M}), \tag{6}$$

and the probability of false negatives is

$$\beta_M := p(H_0|H_1) = \text{Tr}(\Pi_0 \rho_1^{\otimes M}). \tag{7}$$

In the limit of a large number of copies ($M \gg 1$), these probabilities go to zero exponentially, i.e., we have

$$\alpha_M \simeq \frac{1}{2} e^{-\alpha_R M}, \ \beta_M \simeq \frac{1}{2} e^{-\beta_R M}, \tag{8}$$

where the coefficients

$$\alpha_R = -\lim_{M \to +\infty} \frac{1}{M} \ln \alpha_M \ , \tag{9}$$
$$\beta_R = -\lim_{M \to +\infty} \frac{1}{M} \ln \beta_M \ , \tag{10}$$

are called the 'error-exponents' or 'rate limits' [11].

Bob's aim is to maximize the error exponent β_R, so that the error probability of false negatives β_M has the fastest exponential decay to zero. This must be done while controlling the rate of false positives. Here a well known result is the 'quantum Stein lemma' [11] which connects β_R with the quantum relative entropy between the single-copy states ρ_0 and ρ_1. For a large number of copies $M \gg 1$, there is a dichotomic POVM such that the error probability of the false positives is bounded

$$\alpha_M \leq \varepsilon \ \text{ for any } 0 < \varepsilon < 1, \tag{11}$$

and the error probability of false negatives goes to zero with error-exponent

$$\beta_R = S(\rho_0 || \rho_1) = \text{Tr} \rho_0 (\ln \rho_0 - \ln \rho_1). \tag{12}$$

More powerfully, we may use the notion of the QHB [11]. For $M \gg 1$, there is a dichotomic POVM such that the error-exponent of false positives is lower-bounded by a positive parameter

$$\alpha_R \geq r \text{ for any } r > 0, \tag{13}$$

and the error-exponent of false negatives satisfies

$$\beta_R = H(r), \tag{14}$$

where $H(r) \geq 0$ is the QHB defined by

$$H(r) := \sup_{0\leq s<1} P(r,s), \quad P(r,s) := \frac{-r\ s - \ln C_s}{1-s}, \tag{15}$$

where

$$C_s := \mathrm{Tr}(\rho_0^s \rho_1^{1-s}) \tag{16}$$

is the 's-overlap' between the single-copy states ρ_0 and ρ_1. Note that the quantum Hoeffding bound enforces a stronger constraint on false-positives, since these are bounded at the level of the error-exponent and not at the level of the error probability as happens for the quantum relative entropy bound.

III. ASYMMETRIC TESTING WITH PURE STATES

Asymmetric testing becomes very simple when one of the states (or both) is pure. In this case, we can in fact relate the QHB to the quantum fidelity between the two states.

Let us start by considering the case where only one of the states is pure, e.g., $\rho_0 = |\psi_0\rangle\langle\psi_0|$. We can write [19]

$$\inf_s C_s = F(|\psi_0\rangle, \rho_1), \tag{17}$$

where F is the fidelity between $|\psi_0\rangle$ and ρ_1. Eq. (17) implies $C_s \geq F$. By using the latter inequality in Eq. (15), we derive the fidelity-bound

$$H(r) \leq H_F(r) := \sup_{0\leq s<1} \frac{-r\ s - \ln F}{1-s}\ . \tag{18}$$

This bound can be further simplified by explicitly performing the maximization with regard to the parameter s. After a simple calculation we find

$$H_F(r) = \begin{cases} \ln\frac{1}{F}, & \text{for } r \geq \ln\frac{1}{F}\ , \\ \\ +\infty, & \text{for } r < \ln\frac{1}{F}\ , \end{cases} \tag{19}$$

which depends on the comparison between the parameter r and the fidelity F of the two states.

More specifically, in the discrimination of two pure states, we find that the previous fidelity-bound becomes tight

$$H(r) = H_F(r)\ . \tag{20}$$

In fact, for pure states $\rho_0 = |\psi_0\rangle\langle\psi_0|$ and $\rho_1 = |\psi_1\rangle\langle\psi_1|$, and for any $0 < s < 1$, we can write

$$\begin{aligned} C_s &= \mathrm{Tr}(|\psi_0\rangle\langle\psi_0|^s |\psi_1\rangle\langle\psi_1|^{1-s}) = \mathrm{Tr}(|\psi_0\rangle\langle\psi_0|\psi_1\rangle\langle\psi_1|) \\ &= |\langle\psi_0|\psi_1\rangle|^2 = F(|\psi_0\rangle, |\psi_1\rangle). \end{aligned} \tag{21}$$

Therefore we can replace $\ln C_s = \ln F$ in the QHB of Eq. (15), which implies Eq. (20) [20].

IV. ASYMMETRIC TESTING WITH GAUSSIAN STATES

A. Basics of bosonic systems and Gaussian states

A bosonic system of n modes is a quantum system described by a tensor product Hilbert space $\mathcal{H}^{\otimes n}$ and a vector of quadrature operators [21, 22]

$$\hat{\mathbf{x}}^T := (\hat{q}_1, \hat{p}_1, \ldots, \hat{q}_n, \hat{p}_n). \tag{22}$$

These operators satisfy the vectorial commutation relations [23]

$$[\hat{\mathbf{x}}, \hat{\mathbf{x}}^T] := \hat{\mathbf{x}}\hat{\mathbf{x}}^T - (\hat{\mathbf{x}}\hat{\mathbf{x}}^T)^T = 2i\mathbf{\Omega}\ , \tag{23}$$

where $\mathbf{\Omega}$ is the symplectic form, defined as

$$\mathbf{\Omega} := \bigoplus_{k=1}^{n} \begin{pmatrix} 0 & 1 \\ -1 & 0 \end{pmatrix}\ . \tag{24}$$

Correspondingly, a real matrix $\mathbf{S}$ is called 'symplectic' when it preserves $\mathbf{\Omega}$ by congruence, i.e., $\mathbf{S}\mathbf{\Omega}\mathbf{S}^T = \mathbf{\Omega}$.

By definition, we say that a bosonic state ρ is 'Gaussian' when its phase-space Wigner representation is Gaussian [5]. In such a case, we can completely describe the state by means of its first- and second-order statistical moments. These are the mean value or displacement vector $\bar{\mathbf{x}} := \mathrm{Tr}(\hat{\mathbf{x}}\rho)$, and the covariance matrix (CM) $\mathbf{V}$ with generic element

$$V_{ij} = \tfrac{1}{2}\mathrm{Tr}(\{\hat{x}_i, \hat{x}_j\}\rho) - \bar{x}_i\bar{x}_j\ , \tag{25}$$

where $\{,\}$ denotes the anticommutator. The CM is a $2n \times 2n$ real symmetric matrix, which must satisfy the uncertainty principle [5]

$$\mathbf{V} + i\mathbf{\Omega} \geq 0\ . \tag{26}$$

An important tool in the manipulation of Gaussian states is Williamson's theorem [5]: For any CM $\mathbf{V}$, there is a symplectic matrix $\mathbf{S}$ such that

$$\mathbf{V} = \mathbf{S}\mathbf{W}\mathbf{S}^T\ , \tag{27}$$

where

$$\mathbf{W} = \bigoplus_{k=1}^{n} \nu_k \mathbf{I}\ ,\ \mathbf{I} := \begin{pmatrix} 1 & 0 \\ 0 & 1 \end{pmatrix}. \tag{28}$$

The matrix $\mathbf{W}$ is the 'Williamson form' of $\mathbf{V}$, and the set $\{\nu_1, \cdots, \nu_n\}$ is the 'symplectic spectrum' of $\mathbf{V}$. According to the uncertainty principle, each symplectic eigenvalue must satisfy the condition $\nu_k \geq 1$, with $\nu_k = 1$ for all k if and only if the Gaussian state is pure.

B. Computation of the quantum Hoeffding bound

Our goal is to find a general recipe for the calculation of the QHB for Gaussian states. We start from the

general formula in Eq. (15) involving the logarithm of the s-overlap C_s defined in Eq. (16). Given two n-mode Gaussian states, ρ_0 and ρ_1, we can write an explicit Gaussian formula for the s-overlap in terms of their statistical moments $(\bar{\mathbf{x}}_0, \mathbf{V}_0)$ and $(\bar{\mathbf{x}}_1, \mathbf{V}_0)$. This is given by [10, 19]

$$C_s = \frac{\Pi_s}{\sqrt{\det \boldsymbol{\Sigma}_s}} \exp\left[-\frac{\mathbf{d}^T \boldsymbol{\Sigma}_s^{-1} \mathbf{d}}{2}\right], \tag{29}$$

where $\mathbf{d} := \bar{\mathbf{x}}_0 - \bar{\mathbf{x}}_1$ is the difference between the mean values, while Π_s and $\boldsymbol{\Sigma}_s$ depends on the CMs $\mathbf{V}_0$ and $\mathbf{V}_1$. In particular, introducing the two real functions

$$G_s(x) := \frac{2^s}{(x+1)^s - (x-1)^s}, \tag{30}$$

$$\Lambda_s(x) := \frac{(x+1)^s + (x-1)^s}{(x+1)^s - (x-1)^s}, \tag{31}$$

we can write the formulas

$$\Pi_s := 2^n \Pi_{k=1}^n G_s(\nu_k^0) G_{1-s}(\nu_k^1) \ , \tag{32}$$

and

$$\begin{aligned} \boldsymbol{\Sigma}_s := \mathbf{S}_0 \ [\oplus_{k=1}^n \Lambda_s(\nu_k^0)\mathbf{I}] \ \mathbf{S}_0^T \\ + \mathbf{S}_1 \ [\oplus_{k=1}^n \Lambda_{1-s}(\nu_k^1)\mathbf{I}] \ \mathbf{S}_1^T, \end{aligned} \tag{33}$$

where $\{\nu_k^0\}$ and $\{\nu_k^1\}$ are the symplectic spectra of the two states, with $\mathbf{S}_0$ and $\mathbf{S}_1$ being the symplectic matrices which diagonalize the two CMs according to Williamson's theorem, i.e.,

$$\mathbf{V}_0 = \mathbf{S}_0 \ (\oplus_{k=1}^n \nu_k^0 \mathbf{I}) \ \mathbf{S}_0^T, \ \mathbf{V}_1 = \mathbf{S}_1 \ (\oplus_{k=1}^n \nu_k^1 \mathbf{I}) \ \mathbf{S}_1^T. \tag{34}$$

Substituting Eq. (29) into Eq. (15), corresponds to explicitly computing the logarithmic term $\ln C_s$, yielding

$$\ln C_s = \ln \Pi_s - \frac{1}{2}\left\{\ln\det \boldsymbol{\Sigma}_s + \mathbf{d}^T \boldsymbol{\Sigma}_s^{-1} \mathbf{d}\right\} \ . \tag{35}$$

In particular for zero-mean Gaussian states we have $\mathbf{d} = 0$ and the previous expression simplifies to

$$\ln C_s = \ln \Pi_s - \frac{1}{2} \ln\det \boldsymbol{\Sigma}_s \ . \tag{36}$$

C. Other computable bounds

Note that computing the s-overlap C_s and its logarithmic form $\ln C_s$ could be difficult due to the presence of the symplectic matrices, $\mathbf{S}_0$ and $\mathbf{S}_1$, in the term $\boldsymbol{\Sigma}_s$ in Eq. (33). A possible solution is to compute an upper bound, known as the 'Minkowski bound', which is based on the Minkowski determinant inequality [24] and depends only on the two symplectic spectra [10]. Specifically, we have $C_s \leq M_s$, where

$$M_s := 4^n \left[\prod_{k=1}^n \Psi_s(\nu_k^0, \nu_k^1) + \prod_{k=1}^n \Psi_{1-s}(\nu_k^1, \nu_k^0)\right]^{-n}, \tag{37}$$

and

$$\begin{aligned} \Psi_s(x,y) := \{[(x+1)^s + (x-1)^s] \\ \times [(y+1)^{1-s} - (y-1)^{1-s}]\}^{1/n}. \end{aligned} \tag{38}$$

Another easy-to-compute upper bound is the 'Young bound' Y_s, which is based on Young's inequality [25] and satisfies

$$C_s \leq M_s \leq Y_s, \tag{39}$$

where [10]

$$Y_s := 2^n \prod_{k=1}^n \Gamma_s(\nu_k^0)\Gamma_{1-s}(\nu_k^1) \ , \tag{40}$$

and

$$\Gamma_s(x) := \left[(x+1)^{2s} - (x-1)^{2s}\right]^{-\frac{1}{2}} \ . \tag{41}$$

Taking the negative logarithm of Eq. (39), we can write the following inequality for the QHB

$$H(r) \geq H_M(r) \geq H_Y(r), \tag{42}$$

where

$$H_M(r) := \sup_{0\leq s<1} \frac{-r \ s - \ln M_s}{1-s}, \tag{43}$$

$$H_Y(r) := \sup_{0\leq s<1} \frac{-r \ s - \ln Y_s}{1-s}. \tag{44}$$

In the specific case where one of the two Gaussian states is pure, we can compute their fidelity F and apply the upper bound given in Eqs. (18) and (19), which becomes tight when both states are pure [see Eq. (20)]. In particular, for two multimode Gaussian states $\rho_0 = |\psi_0\rangle\langle\psi_0|$ and ρ_1, we can easily write their fidelity F in terms of the statistical moments [19]

$$F = \frac{2^n}{\sqrt{\det \mathbf{L}}} \exp\left(-\frac{\mathbf{d}^T \mathbf{L}^{-1} \mathbf{d}}{2}\right), \tag{45}$$

where $\mathbf{L} := \mathbf{V}_0 + \mathbf{V}_1$. As a result, we can use Eq. (19) with

$$\ln \frac{1}{F} = \frac{1}{2}\left[\ln\left(\frac{\det \mathbf{L}}{4^n}\right) + \mathbf{d}^T \mathbf{L}^{-1} \mathbf{d}\right]. \tag{46}$$

V. DISCRIMINATION OF ONE-MODE GAUSSIAN STATES

In this section, we examine the case of one-mode Gaussian states. This means we fix $n = 1$ in the previous formulas of Sec. IV, with matrices becoming 2×2, vectors becoming 2-dimensional, and symplectic spectra reducing to a single eigenvalue. For instance, the s-overlap can be more simply computed using the expressions

$$\Pi_s = 2 \ G_s(\nu^0) \ G_{1-s}(\nu^1), \tag{47}$$

$$\boldsymbol{\Sigma}_s = \Lambda_s(\nu^0) \ \mathbf{S}_0 \mathbf{S}_0^T + \Lambda_{1-s}(\nu^1) \ \mathbf{S}_1 \mathbf{S}_1^T. \tag{48}$$

In particular, here we shall derive the analytic formulas for the QHB for two important classes: Coherent states (in Sec. V A) and thermal states (in Sec. V B).

A. Asymmetric testing of coherent amplitudes

The expression of the QHB is greatly simplified in the case of one-mode coherent states $\rho_0 = |\alpha_0\rangle\langle\alpha_0|$ and $\rho_1 = |\alpha_1\rangle\langle\alpha_1|$. Since both states are pure, the QHB is equal to the fidelity bound in Eq. (19), i.e., $H(r) = H_F(r)$. Therefore, it is sufficient to compute the fidelity between the two coherent states, which is given by

$$F = |\langle\alpha_0|\,\alpha_1\rangle|^2 = e^{-|\alpha_0-\alpha_1|^2}, \tag{49}$$

so that $\ln\frac{1}{F} = |\alpha_0 - \alpha_1|^2 := \sigma$, and we can write

$$H(r) = \begin{cases} \sigma\ , & \text{for } r \geq \sigma\ , \\ \\ +\infty\ , & \text{for } r < \sigma\ . \end{cases} \tag{50}$$

Assuming that we impose a good control on the rate of false positives (so that $r \geq \sigma$), then the error-exponent for the false negatives is simply given by $H(r) = \sigma$. More explicitly, this corresponds to an asymptotic error rate

$$\beta_M = \frac{1}{2}e^{-M\sigma} = \frac{F^M}{2}\ . \tag{51}$$

Note that, if we have poor control on the rate of false positives, i.e., $r < \sigma$, then the QHB $H(r)$ is infinite. This means that the probability of false negatives β_M goes to zero super-exponentially, i.e., more quickly than any decreasing exponential function.

B. Asymmetric testing of thermal noise

In this section we derive the QHB for one-mode thermal states $\rho_0 = \rho_{\rm th}(\nu^0)$ and $\rho_1 = \rho_{\rm th}(\nu^1)$, with variances equal to ν^0 and ν^1, respectively (in our notation, $\nu = 2\bar{n} + 1$, where $\bar{n}$ is the mean number of thermal photons). These Gaussian states have zero mean ($\bar{\mathbf{x}}_0 = \bar{\mathbf{x}}_1 = 0$) and CMs in the Williamson form $\mathbf{V}_0 = \nu^0\mathbf{I}$ and $\mathbf{V}_1 = \nu^1\mathbf{I}$ (so that $\mathbf{S}_0 = \mathbf{S}_1 = \mathbf{I}$). Thus, we can write

$$\mathbf{\Sigma}_s = \varepsilon_s\mathbf{I},\ \varepsilon_s := \Lambda_s(\nu^0) + \Lambda_{1-s}(\nu^1), \tag{52}$$

and derive

$$C_s = \frac{\Pi_s}{\varepsilon_s} = \frac{2}{(\nu^0+1)^s(\nu^1+1)^{1-s} - (\nu^0-1)^s(\nu^1-1)^{1-s}}. \tag{53}$$

This is the s-overlap to be used in the QHB of Eq. (15).

Given two arbitrary $\nu^0 \geq 1$ and $\nu^1 \geq 1$, the maximization in Eq. (15) can be done numerically. The results are shown in Fig. 1 for thermal states with variances up to 3 vacuum units (equivalent to 1 mean thermal photon). From the figure we can see an asymmetry with respect to the bisector $\nu^0 = \nu^1$ which is a consequence of the asymmetric nature of the hypothesis test. The bottom-right part of the figure is related to the minimum probability of confusing a nearly-vacuum state ($\nu^1 \simeq 1$) with a thermal state having one average photon ($\nu^0 \simeq 3$). By contrast, the top-left part of the figure is related to the probability of confusing a thermal state having one average photon ($\nu^1 \simeq 3$) with a nearly-vacuum state ($\nu^0 \simeq 1$). These probabilities are clearly different.

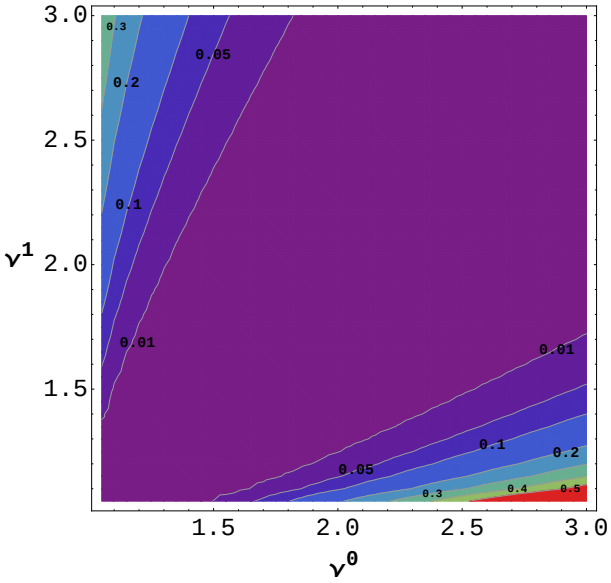

FIG. 1: (Color online). We plot the QHB associated with the discrimination of two thermal states: $\rho_{\rm th}(\nu^0)$ as null hypothesis, and $\rho_{\rm th}(\nu^1)$ as alternative hypothesis. We consider low thermal variances $1 < \nu^0, \nu^1 \leq 3$ and we have set $r = 0.1$ for the false positives.

We are able to derive a simple analytical result when we compare a thermal state with the vacuum state. Let us start by considering the vacuum state to be the null hypothesis ($\nu^0 = 1$) while the thermal state is the alternative hypothesis ($\nu^1 := \nu > 1$). In this specific case, we find

$$\ln C_s = (1-s)\ln\left(\frac{2}{1+\nu}\right)\ , \tag{54}$$

and we get

$$P(r,s) = \ln\left(\frac{1+\nu}{2}\right) - \frac{rs}{1-s}\ . \tag{55}$$

Since ν is a constant, the maximization of P over $0 \leq s < 1$ corresponds to minimizing the function $rs(1-s)^{-1}$, whose minimum occurs at $s = 0$. As a result, we have

$$H(r) = P(r,0) = \ln\left(\frac{1+\nu}{2}\right).$$

Since $\nu = 2\bar{n} + 1$, we can write the QHB in terms of the mean number of thermal photons, i.e.,

$$H(r) = \ln(\bar{n}+1). \tag{56}$$

This is the optimal error exponent for the asymptotic probability of false negatives, i.e., of confusing a thermal state with the vacuum state.

Let us now consider the thermal state to be the null hypothesis ($\nu^0 := \nu > 1$) while the vacuum state is the alternative hypothesis ($\nu^1 = 1$). In this case, we derive

$$P(r,s) = \frac{s}{1-s}\left[\ln\left(\frac{1+\nu}{2}\right) - r\right], \tag{57}$$

which leads to the following expression for the QHB

$$H(r) = \begin{cases} 0 & \text{for } r \geq \ln\left(\frac{1+\nu}{2}\right) \\ +\infty & \text{for } r < \ln\left(\frac{1+\nu}{2}\right) \end{cases}. \tag{58}$$

This is related to the minimum probability of confusing the vacuum state with a thermal state. Note that this is very different from Eq. (56).

VI. DISCRIMINATION OF TWO-MODE GAUSSIAN STATES

In this section we consider two important classes of two-mode Gaussian states. The first is the class of Einstein-Podolsky-Rosen (EPR) states, also known as two-mode squeezed vacuum states. The second (broader) class is that of two-mode squeezed thermal (ST) states, for which the computation of the QHB is numerical.

A. Asymmetric testing of EPR correlations

The expression of the QHB in the case of EPR states is easy to derive. Since EPR states are pure, the QHB $H(r)$ is given by $H_F(r)$ of Eq. (19). As a result, we need only to compute the fidelity between the two states.

An EPR state has zero mean and CM

$$\mathbf{V}_{\rm EPR}(\mu) = \begin{pmatrix} \mu\mathbf{I} & \sqrt{\mu^2-1}\mathbf{Z} \\ \sqrt{\mu^2-1}\mathbf{Z} & \mu\mathbf{I} \end{pmatrix}, \tag{59}$$

with $\mu \geq 1$, $\mathbf{I}$ is the 2×2 identity matrix and

$$\mathbf{Z} := \begin{pmatrix} 1 & 0 \\ 0 & -1 \end{pmatrix}. \tag{60}$$

Given two EPR states with parameters μ_0 and μ_1, their fidelity is computed via Eq. (45), yielding

$$F = \frac{4}{\sqrt{\det \mathbf{L}}}, \tag{61}$$

where $\mathbf{L} = \mathbf{V}_{\rm EPR}(\mu_0) + \mathbf{V}_{\rm EPR}(\mu_1)$. After simple algebra, we find

$$F = \frac{2}{1+\mu_0\mu_1 - \sqrt{(\mu_0^2-1)(\mu_1^2-1)}}, \tag{62}$$

to be used in Eq. (19).

B. Squeezed thermal states

In this section we consider symmetric ST states $\rho(\mu, c)$, which are Gaussian states with zero mean and CM

$$\mathbf{V}_{\rm ST}(\mu, c) = \begin{pmatrix} \mu\mathbf{I} & c\mathbf{Z} \\ c\mathbf{Z} & \mu\mathbf{I} \end{pmatrix}, \tag{63}$$

where $\mu \geq 1$ and $|c| \leq \mu$ [26, 27] (in particular, without loss of generality, we can assume $c \geq 0$). These are called symmetric because they are invariant under permutation of the two modes [28].

Note that, for $c = 0$, we have no correlations, and the ST state is a tensor-product of thermal states, i.e., $\rho(\mu, 0) = \rho_{\rm th}(\mu)^{\otimes 2}$. For $c = \sqrt{\mu^2-1}$ the correlations are maximal, and the ST state becomes an EPR state, i.e., $\rho(\mu, \sqrt{\mu^2-1}) = \rho_{\rm EPR}(\mu)$. Finally, for $c = \mu - 1$, we have maximal separable correlations. In other words, $\rho(\mu, \mu-1)$ is the separable ST state with the strongest correlations (e.g., highest discord).

The symplectic decomposition of a symmetric ST state is known. From the CM of Eq. (63), one can check that the symplectic spectrum is degenerate and given by the single eigenvalue

$$\nu = \sqrt{\mu^2 - c^2}. \tag{64}$$

The symplectic matrix $\mathbf{S}$ which diagonalizes $\mathbf{V}_{\rm ST}(\mu, c)$ in Williamson form $\nu(\mathbf{I}\oplus\mathbf{I})$ is given by

$$\mathbf{S} = \begin{pmatrix} \omega_+\mathbf{I} & \omega_-\mathbf{Z} \\ \omega_-\mathbf{Z} & \omega_+\mathbf{I} \end{pmatrix}, \tag{65}$$

where

$$\omega_\pm := \sqrt{\frac{\mu \pm \nu}{2\nu}}. \tag{66}$$

As a result, the s-overlap between two symmetric ST states, ρ_0 and ρ_1, can be computed using the simplified formulas

$$\Pi_s = 4\; G_s^2(\nu^0)\; G_{1-s}^2(\nu^1), \tag{67}$$

$$\mathbf{\Sigma}_s = \Lambda_s(\nu^0)\; \mathbf{S}_0\mathbf{S}_0^T + \Lambda_{1-s}(\nu^1)\; \mathbf{S}_1\mathbf{S}_1^T, \tag{68}$$

where ν^0 (ν^1) is the degenerate eigenvalue of ρ_0 (ρ_1), computed according to Eq. (64), and $\mathbf{S}_0$ ($\mathbf{S}_1$) is the corresponding diagonalizing symplectic matrix, computed according to Eqs. (65) and (66).

Let us start with simple cases involving the asymmetric testing of correlations with specific ST states. First we consider the asymmetric discrimination between the uncorrelated thermal state $\rho_0 = \rho(\mu, 0)$ as null hypothesis and the correlated (but separable) ST state $\rho_1 = \rho(\mu, \mu-1)$ as alternative hypothesis. A false negative corresponds to concluding that there are no correlations where they are actually present [29]. It is straightforward to derive their degenerate symplectic eigenvalues which are simply $\nu^0 = \mu$ and $\nu^1 = \sqrt{2\mu-1}$. Then, we have $\mathbf{S}_0 = \mathbf{I}\oplus\mathbf{I}$,

while $\mathbf{S}_1$ can be easily computed from Eqs. (65) and (66). By substituting these into Eqs. (67) and (68), we can compute the s-overlap $C_s = \Pi_s/\sqrt{\det \mathbf{\Sigma}_s}$ and therefore the QHB $H(r)$ via Eq. (15). The results are plotted in Fig. 2, for values of thermal variance μ up to 3 (i.e., from zero to 1 mean photon) and small values of the parameter r, bounding the rate of false-positives. As expected, the QHB improves for decreasing r and increasing μ.

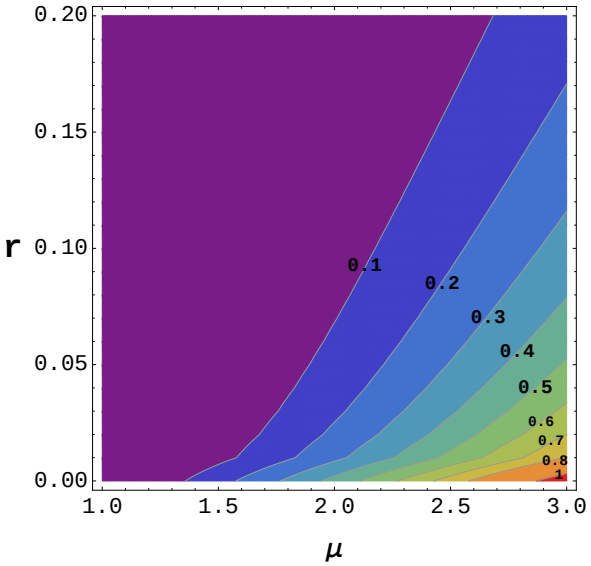

FIG. 2: (Color online). Asymmetric discrimination between the thermal state $\rho_0 = \rho(\mu, 0)$ and the ST state $\rho_1 = \rho(\mu, \mu - 1)$ with maximal separable correlations. We plot the QHB as a function of the thermal variance μ and the false-positive parameter r. As we can see the QHB improves for lower r and for higher μ.

Now let us consider the asymmetric discrimination between $\rho_0 = \rho(\mu, 0)$ and the EPR state $\rho_1 = \rho_{\text{EPR}}(\mu)$, i.e., the most correlated and entangled ST state [29]. Thanks to the simple symplectic decomposition of the EPR state ($\nu^1 = 1$), we can further simplify the previous Eqs. (67)-(68) and write

$$\Pi_s = 4\, G_s^2(\mu),\ \mathbf{\Sigma}_s = \Lambda_s(\mu)\ (\mathbf{I} \oplus \mathbf{I}) + \mathbf{V}_{\text{EPR}}(\mu), \quad (69)$$

with $\mathbf{V}_{\text{EPR}}(\mu)$ being given by Eq. (59). As before, we compute the QHB which is plotted in Fig. 3, for $1 \leq \mu \leq 3$ and $r \leq 2$. As expected the QHB improves for decreasing r and increasing μ. Note a discontinuity identifying two regions, one where the QHB is finite, and the other where it is infinite (white region in the figure).

In fact, by expanding the term $P(r, s)$ in Eq. (15) for $s \to 1^-$, that we find

$$P(r, s) \simeq \frac{N}{s - 1} + O(s - 1), \quad (70)$$

where

$$N := r - \ln\left(\frac{1 + 3\mu^2}{4}\right). \quad (71)$$

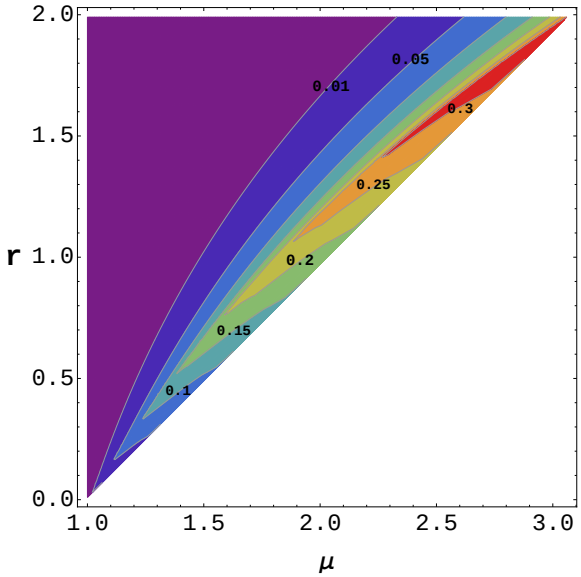

FIG. 3: (Color online). Asymmetric discrimination between the thermal state $\rho_0 = \rho(\mu, 0)$ and the EPR state $\rho_1 = \rho_{\text{EPR}}(\mu)$. We plot the QHB as a function of the thermal variance μ and the false-positive parameter r. The QHB improves for lower r and for higher μ. In particular, there is a threshold value after which the QHB becomes infinite (white region).

For values of r and μ such that $N > 0$, we find that the term $P(r, s)$ diverges at the border, making the QHB infinite. For a given r, this happens when

$$\mu > \tilde{\mu}(r) := \sqrt{\frac{4e^r - 1}{3}}. \quad (72)$$

Finally, we consider the most general scenario in the asymmetric testing of correlations with ST states. In fact, we consider two generic ST states, $\rho(\mu, c_0)$ and $\rho(\mu, c_1)$, with the same thermal noise but differing amounts of correlation. For this computation, we use Eqs. (64)-(66) with $c = c_0$ or c_1, to be replaced in Eqs. (67)-(68), therefore deriving the s-overlap and the QHB. At small thermal variance ($\mu = 3$) and for the numerical value $r = 0.1$, we plot the QHB as a function of the correlation parameters c_0 and c_1. As we can see from Fig. 4, the QHB is not symmetric with respect to the bisector $c_0 = c_1$ (where it is zero) and increases away from this line.

VII. CONCLUSION

In this work we have considered the problem of asymmetric quantum hypothesis testing by adopting the recently-developed tool of the quantum Hoeffding bound (QHB). After a brief review of these notions, we have shown how the QHB can be simplified in some cases (pure states) and estimated using other easier-to-compute bounds based on simple algebraic inequalities.

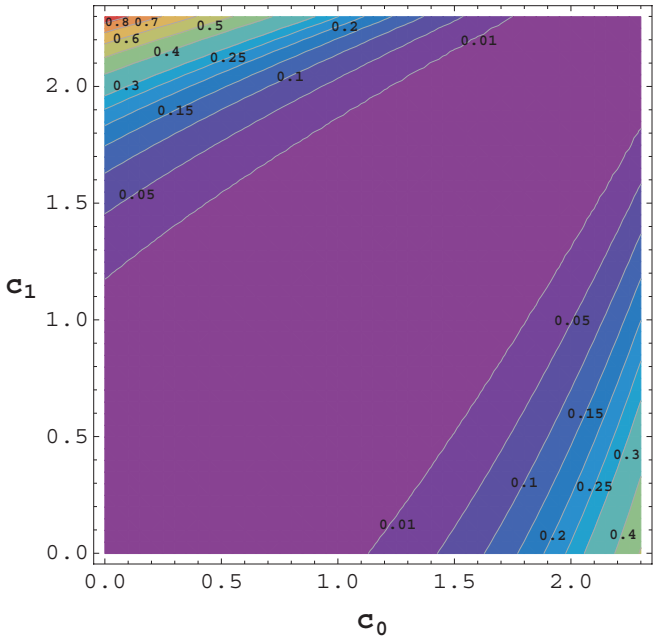

FIG. 4: (Color online). Asymmetric discrimination between two ST states with the same thermal variance ($\mu = 3$) but different correlations c_0 and c_1. Setting $r = 0.1$, we plot the QHB as a function of c_0 and c_1. We can see that the QHB increases orthogonally to the bisector $c_0 = c_1$.

In particular, we have applied the theory of asymmetric testing to multimode Gaussian states, providing a general recipe for the computation of the QHB in the Gaussian setting. Using this recipe, we have found analytic formulas and shown numerical results for important classes of one-mode and two-mode Gaussian states. In particular, we have studied the behavior of the QHB in the low energy regime, i.e., considering Gaussian states with a small average number of photons.

Our results could be exploited in protocols of quantum information with continuous variables. In particular, they could be useful for reformulating Gaussian schemes of quantum state discrimination and quantum channel discrimination in such a way as to give more importance to one of the quantum hypotheses. This asymmetric approach could be the most suitable in the development of quantum technology for medical applications.

Acknowledgments

This work has been supported by EPSRC (EP/J00796X/1). G.S. has been supported by an EPSRC DTA grant. The authors thank C. Ottaviani and S. Pirandola for enlightening discussions.

[1] M. M. Wilde, *Quantum Information Theory* (Cambridge University Press, Cambridge, 2013).
[2] M. A. Nielsen and I. L. Chuang, *Quantum Computation and Quantum Information* (Cambridge University Press 2000).
[3] C. Silberhorn, T. C. Ralph, N. Lutkenhaus, and G. Leuchs, Phys. Rev. Lett. **89**, 167901 (2002).
[4] A. M. Lance, T. Symul, V. Sharma, C. Weedbrook, T. C. Ralph, and P. K. Lam, Phys. Rev. Lett. **95**, 180503 (2005).
[5] C. Weedbrook, S. Pirandola, R. Garcia-Patron, N. J. Cerf, T. C. Ralph, J. H. Shapiro, and S. Lloyd, Rev. Mod. Phys. **84**, 621 (2012).
[6] C. W. Helstrom, *Quantum Detection and Estimation Theory*, *Mathematics in Science and Engineering*, Vol. 123 (Academic Press, New York, 1976).
[7] A. Chefles, Contemp. Phys. **41**, 401 (2000).
[8] S. M. Barnett and S. Croke, Advances in Optics and Photonics **1**, 238-278 (2009).
[9] K. M. R. Audenaert, J. Calsamiglia, L. Masanes, R. Munoz-Tapia, A. Acın, E. Bagan, and F. Verstraete, Phys. Rev. Lett. **98**, 160501 (2007).
[10] S. Pirandola, and S. Lloyd, Phys. Rev. A **78**, 012331 (2008).
[11] K. M. R. Audenaert, M. Nussbaum, A. Szkola, and F. Verstraete, Commun. Math. Phys. **279**, 251 (2008).
[12] R. Jozsa, J. Mod. Opt. **41**, 2315 (1994).
[13] S.-H. Tan, B. I. Erkmen, V. Giovannetti, S. Guha, S. Lloyd, L. Maccone, S. Pirandola, and J. H. Shapiro, Phys. Rev. Lett. **101**, 253601 (2008).
[14] S. Lloyd, Science **321**, 1463 (2008).
[15] S. Pirandola, Phys. Rev. Lett. **106**, 090504 (2011).
[16] S. Pirandola, C. Lupo, V. Giovannetti, S. Mancini, and S. L. Braunstein, New J. Phys. **13**, 113012 (2011).
[17] G. Spedalieri, C. Lupo, S. Mancini, S. L. Braunstein, and S. Pirandola, Phys. Rev. A **86**, 012315 (2012).
[18] C. Lupo, S. Pirandola, V. Giovannetti, and S. Mancini, Phys. Rev. A **87**, 062310 (2013).
[19] G. Spedalieri, C. Weedbrook, and S. Pirandola, J. Phys. A: Math. Theor. **46**, 025304 (2013).
[20] We can write $H(r) = \max\{P(r,0), \sup_{0<s<1} P(r,s)\}$, where $P(r,0) = -\ln C_0 = 0$ can be neglected and

$$\sup_{0<s<1} P(r,s) = \sup_{0<s<1} \frac{-r\ s - \ln F}{1-s} = \begin{cases} \ln \frac{1}{F} & \text{for } r \geq \ln \frac{1}{F}, \\ +\infty & \text{for } r < \ln \frac{1}{F}. \end{cases}$$

[21] S. L. Braunstein, and P. van Loock, Rev. Mod. Phys. **77**, 513 (2005).
[22] S. L. Braunstein, and A. K. Pati, *Quantum Information with Continuous Variables* (Kluwer Academic, Dordrecht, 2003).
[23] More generally, for any two vectorial operators $\mathbf{a}$ and $\mathbf{b}$, we can express their commutation relations in the compact form $[\mathbf{a}, \mathbf{b}^T] := \mathbf{a}\mathbf{b}^T - (\mathbf{b}\mathbf{a}^T)^T$.
[24] R. Bhatia, *Matrix Analysis* (Springer-Verlag, New York, 1997).
[25] W. H. Young, Proc. R. Soc. London, Ser. A **87**, 331 (1912).
[26] S. Pirandola, A. Serafini, and S. Lloyd, Phys. Rev. A **79**, 052327 (2009).
[27] S. Pirandola, New J. Phys. **15**, 113046 (2013).
[28] Extension to asymmetric ST states is only technical.

[29] For brevity we do not consider the other case where the ST state is the null hypothesis and the thermal state is the alternative hypothesis. This case is included in the our final analysis for generic ST states.